AIMS Geosciences, 11(2): 370–386.
DOI: 10.3934/geosci.2025016
Received: 30 October 2024
Revised: 13 March 2025
Accepted: 09 April 2025
Published: 06 May 2025

https://www.aimspress.com/journal/geosciences

*Case report*

# Effects of the Guando Slump on the tectonic interpretation of the Boquerón Thrust in the Guando oilfield [Tolima, Colombia]

**Eduardo Antonio Rossello***

Departamento de Ciencias Geológicas, Consejo Nacional de Investigaciones Científicas y Técnicas [CONICET] – Instituto de Geología y Ciencias Básicas de Buenos Aires [IGEBA], Facultad de Ciencias Exactas y Naturales, Universidad de Buenos Aires, Pabellón II, Ciudad Universitaria [1428] Buenos Aires, Argentina

* **Correspondence:** Email: ea_rossello@yahoo.com.ar.

**Abstract:** A detailed geological study of the Guando oilfield has identified a modern landslide phenomenon that significantly alters the previous structural model and affects production challenges. The multi-compositional nature of the oil-bearing Cretaceous sequences of the Villeta Group, the rugged relief, the climatic incidence, and seismic activity in the Upper Magdalena Valley trigger the Guando Slump, which adjusts the topography to levels of greater stability. The previous tectonic model of the Guando oilfield was based on the superposition of an internally disturbed block by the Boquerón thrust. However, in its westernmost segment, this structure shows angular incompatibilities with the expected horizontal stress fields. Therefore, based on a detailed 3D interpretation of geological maps, DEM, and available geophysical data, we propose that this segment must be associated with the surface of the underlying detachment of the Guando Slump. The horizontal displacement of the landslide, ranging from 1 to 2 km, deforms and collapses the wells that reach the underlying productive reservoirs. This study describes the relationship of this new tectonic model of the Guando oilfield, considering the westernmost segment of the Boquerón thrust as a detachment of the Guando Slump. This real-life example, if properly monitored, will contribute to a better management of the possible causes and consequences of technical problems encountered in the Guando oilfield exploration and prevent catastrophic risks to the production facilities.

**Keywords**: Gravitational landslide; structural control; tectonics; Guando oilfield; Colombia

## 1. Introduction

The Guando Slump is located above the Guando oilfield in the northeastern end of the Girardot sub-basin within the northern part of the Upper Magdalena Valley Basin [1–8]. Virtually all of the producing wells in the oilfield pass through the Guando Slump to reach the main reservoir levels of the Cretaceous sequences (Figure 1).

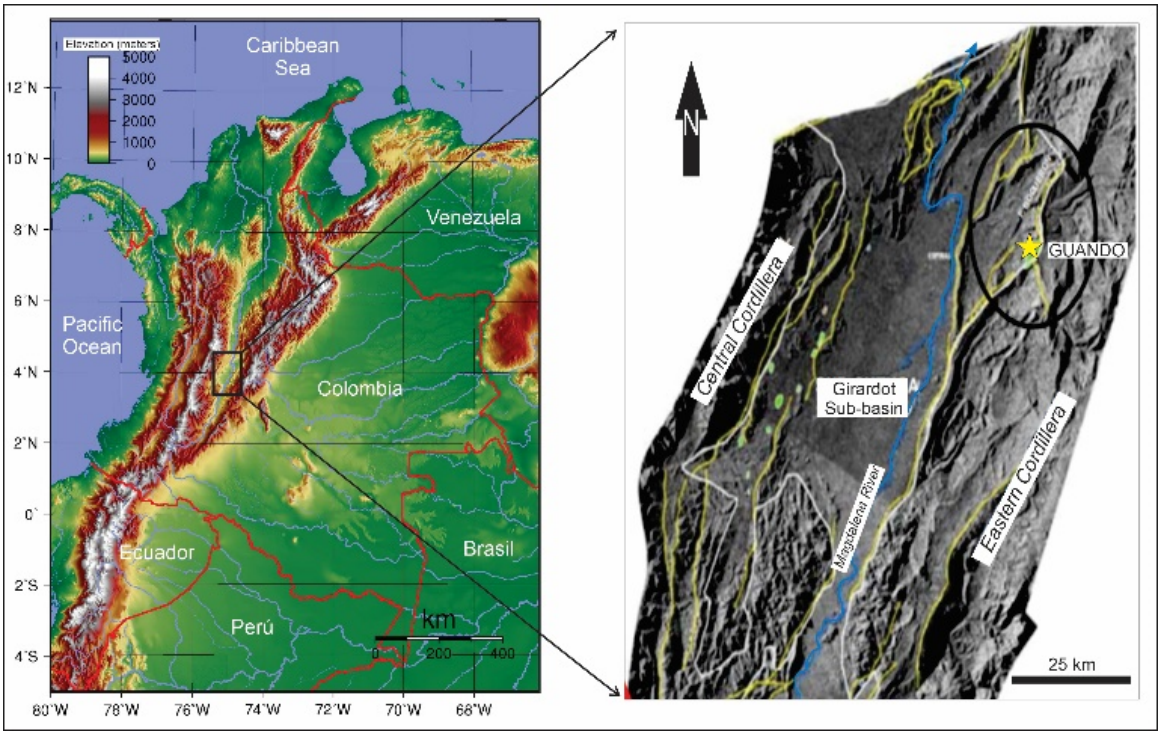


**Figure 1.** Location of the Guando Slump in the Girardot sub-basin of the Upper Magdalena Valley, in the Tolima Department of Colombia, based on regional topographic and RADAR maps.

The Guando oilfield is underlain by a large gravity slip that obscures the structural understanding of its component sedimentary sequences [1]. Previous interpretations have linked low-angle faulting to produced repeats and displacements to the Boquerón thrust. However, they cannot be linked to the characteristic Andean transpressional tectonics responsible for the conformation of the Upper Magdalena Valley. The area within which it is located, on the western flank of the Eastern Cordillera of Colombia, is considered to have a high risk of landslide hazard due to the dominant topographic and climatic characteristics [9]. The geomorphology of the studied sector is dominated by a semicircular depression open to the west, extensively vegetated, where the slope created by the collapsing outcrop is prominent (Figure 2).

The previous structural model of the Guando oilfield was based mainly on the application of 2D geometric balanced reconstruction techniques through the Boquerón thrust. However, the influence of the gravitational slip due to the Guando Slump has been largely neglected. Therefore, current theoretical and practical analysis of the available geological, topographical, and geophysical data

makes it possible to propose a new tectonic model capable of explaining the spatial arrangement of the oil-producing horizons and a better-adapted correlation with the Boquerón thrust.


**Figure 2.** Photographs. **A**. Northeast view showing the topographic ridge marking the eastern boundary of the Guando Slump. **B**. South view showing in the foreground the steep slope of the escarpment and the position of an oil-production well (open arrow) on a block of the landslide. **C**. View to the north of the Guadalupe Formation sandstone scarp.

Previously, Rossello and Saavedra [8] carried out a structural study of the available surface and subsurface geological information of the Guando oilfield, with particular emphasis on the analysis of the Boquerón thrust. DEM and RADAR imagery combined with the reinterpretation of a 3D seismic survey and well controls have led to the recognition of the modern Guando Slump phenomenon. This gravitational sliding significantly modifies the previously known structural model based on the low-angle faulting, superposing Villeta Group levels on younger strata.

The aim of this paper is to describe the main morpho-structural features of the gravity displacements superimposed on the Boquerón thrust in the Guando oilfield, as an example that can be extrapolated to situations with similar structural environments. The Guando Slump provided an example of the characteristic geoforms of gravity displacements and their possible causes and consequences for exploration activities (Figure 1). Therefore, a new structural model of the Guando oilfield is proposed, which takes into account the integral characteristics of the Boquerón thrust and

the recent deformation events due to the Guando landslide. The understanding of this new tectonic model is not only useful to explain the constant collapse problems of the producing wells but also to predict future events with mitigation tasks.

## 2. Materials and methodology

In the structural interpretation of mountainous areas as a result of compressional tectonic convergence, it is very common to consider thrusting as the main responsible factor for the generation of relief, both by models of thick or thin tectonics [10]. Moreover, as a consequence of the instability of their slopes, they usually show phenomena of landslides or shallow gravity movements [11–20].

Thus, the slopes of the relief are attenuated by achieving conditions of greater stability by adapting to the base levels [21]. In this way, the conventional tectonic interpretation is often influenced and erased by features attributed to more recent gravity-like phenomena. On the other hand, when these sectors are located on exploration targets, the stability of the logistical installations is affected and, in the case of the wells that pass through them, the risks described [22,23] include blockages and collapses due to the displacements and modifications of the terrain that occur on the sub-horizontal surfaces of the displacement.

A synthesis of the tectonic evolution of the sector was undertaken to describe and interpret the Guando Slump and its implications for structural interpretation. The available subsurface information was integrated in 3D with the topographic and geological surface mapping according to the criteria of [24]. In order to conceptualize the main characteristics of the gravity slip processes, a compilation of theoretical aspects of their morphologies and generation processes was carried out, using analogies to classical real cases extracted from specific literature [14–22].

The geomorphological interpretation was carried out using high-precision digital elevation models (3601 × 3601 pixels with a spatial resolution of 1 arcsecond) from the open-source satellite imaging program SRTM (Shuttle Radar Topography Mission) using ArcGIS. The analysis of the seismic and well data was carried out using industrial software on a workstation kindly provided by Petrobras Colombia. This topography was acquired and overlaid with regional geological mapping. Due to the excellent evidence provided by digital mapping, visualizations of block diagrams and profiles were obtained with different orientations, highlighted with artificial shading to facilitate the geomorphological interpretation [25].

A brief review of the geological history of the Upper Magdalena Valley Basin, focusing on the tectonic evolution, is given to analyze the impact of the Guando Slump on the conventional structural interpretation of the subsurface oil field. In order to describe the geometry of the slump at depth and to estimate its evolution, 4D models have been constructed, supported by transects fitted with acquisitions of the available reflection seismic data previously studied by [8].

## 3. Geological setting

The Guando field covers an area of 60 $km^2$ at an average altitude of 1300 m a.s.l. It has more than 143 wells, of which approximately 109 produce oil, with an average production of approximately 20,000 BPD of light oil (29.5° API), 50,000 BPD of water, and 2000 KPC of gas (Figure 3). It was discovered in the year 2000 and has significant reserves estimated at 130 MMBO. The structural model is characterized by a sub-thrust trap associated with the Boquerón thrust system, which marks the

boundary between the Upper Magdalena Valley and the Eastern Cordillera (Figure 3). The producing horizon is the Guadalupe Formation with average depths of 1200 m and average pressures of about 300 psi. The source rocks are pelites and marly limestones of the Villeta Group of Late Albian to Santonian age, and it is postulated that the oil kitchens are derived from the nearest synclines. The Guaduas Formation is composed of clays and small sandy intercalations (Figure 4).

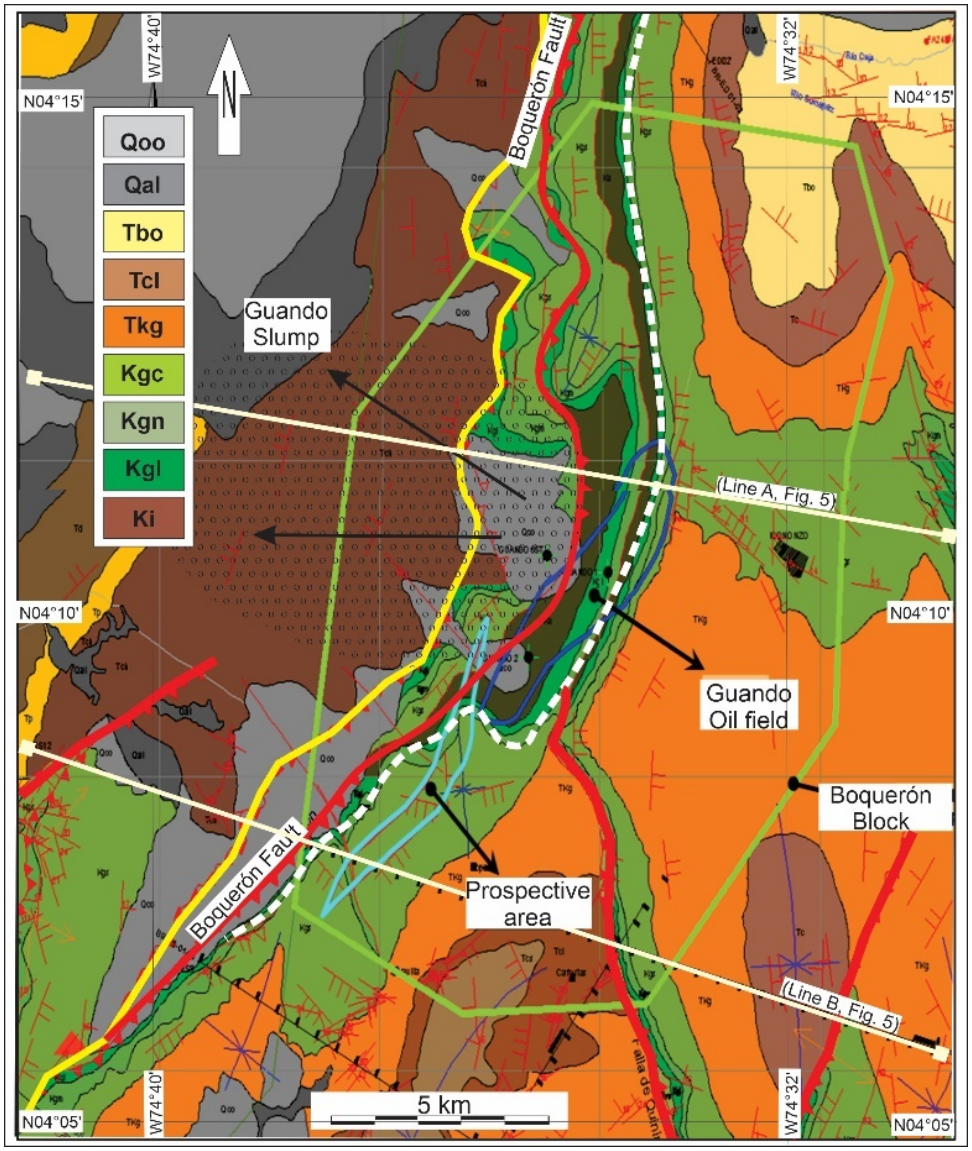


**Figure 3**. Location of the Guando oilfield in the VSM on a regional geological map. Horizontal dashed area indicates outcrops disturbed by gravity sliding from the head (white dashed line) and the western boundary (yellow line). The red line indicates the outcrop of the main faults (Ki: Saldaña-Yavi Formation; Kgl: F: Caballos Formation, Kgn: Villeta Group, Kgc: Monserrate Formation, Tkg: Guadala Formation, Tcl: Barzalosa F., Tbo: Orteguaza F., Qal: Alluvial deposits, Qoo: modern sediments). The green polygon indicates the Guando oilfield license. The blue polygons show the underlying producing areas (modified from [8]).

*3.1. Stratigraphy*

The stratigraphy of the Guando area has been adapted from the Upper Magdalena Valley Basin [26,27]. To describe the main sedimentary records, it can be divided into the following three main depositional sequences (Figure 4):

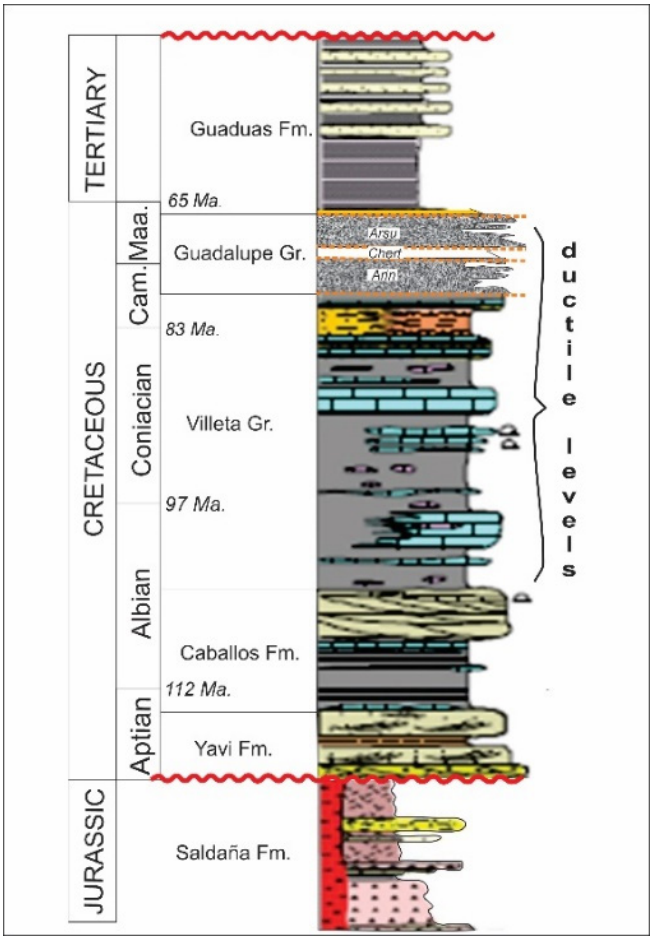


**Figure 4**. Stratigraphic map of the Guando Field showing interbedded ductile levels of the Villeta and Guadalupe Groups as potential triggers for the Guando Slump detachment levels.

(a) Triassic rhyolitic volcaniclastic of the Saldaña Formation overlying a Paleozoic crystalline basement [28,29]. The thickness of the Triassic-Neogene sedimentary sequence is up to 9000 m thick, and its deposition was at least partly controlled by pre-existing Paleozoic extensional faults.

(b) Cretaceous non-marine clastics (Saldaña-Yavi and Caballos formations, and Guadalupe Gr.) to marine and carbonates (Villeta Gr.), influenced by successive phases of the Andean orogeny, starting with the mid-Cretaceous Peruvian phase [30].

(c) Tertiary non-marine molasse succession (Guaduas Fm.) associated with the deformation and major uplifts of the Eastern Cordillera, causing exhumation, erosion, and the subsequent deposition of thicker continental sediments.

### *3.2. Tectonic framework*

From the point of view of regional tectonic analysis, the Upper Magdalena Valley (OMV) is a typical ramp basin (in the sense of [30]), with a multi-phase history, mainly influenced by the different phases of Andean tectonics. As a result, it is bounded by major thrusting to the west by the Cordillera Central and to the east by the Cordillera Oriental [29,31–33].

The main tectonic stages that have affected the region, based on surface and subsurface data and our own interpretations, have been compiled from the abundant related literature [4,22,34]. Although the tectonic history of the VSM basin began in the Triassic-Jurassic as a back-arc depocenter, it may have been at least partially controlled by pre-existing Paleozoic anisotropies [35]. The morphotectonic conformation of the studied area has been acquired from the Neogene to the present by the Andean tectonics, with the deposition of syntectonic sediments in intermontane basins.

The following three Andean phases, due to the convergence of the Nazca plate with the South American plate, are mainly responsible for the structural features expressed in the seismic data associated with the development of petroleum systems in several fields in the region [26, among others].

a) The Peruvian Phase or "Mochica Event": generally, poorly recognized in Colombia, although well represented in the rest of the Andes [36]; in the VSM, it is bounded by the Albian-Cenomanian with a main direction of WSW-ENE compression [26].

b) The Incaic Phase, widely recognized in the Upper Magdalena Valley Basin, started in the Early Eocene and reached its climax in the Middle Eocene [31,32,36]. It started with an increase in the convergence between the Nazca and South American plates. Their convergence determines the cortical shortening structures expressed by widespread distributed thrusts involving the basement, especially on the western and eastern margins of the Cordillera Central.

c) The Quechua Phase: with several deformational episodes during the Neogene. During this phase, the Boquerón thrust (among others), syntectonically associated with folds with axes arranged in directions preferentially perpendicular to the main direction of WSW-ENE convergence [26], is the main feature of the Boquerón thrust. As a result of the Quechua phase of the Andean orogeny between the Late Miocene and the present, the Eastern Cordillera was compressed and uplifted with the development of the basement-involved Boquerón thrust system [36,37]. Folds with NNE-SSW oriented axes suggest WSW-ENE compression during the Middle Miocene. During the Pliocene, NW-SE strike-slip faulting involving the basement displaced fold axes and pre-existing faults [31,32].

### *3.3. Previous tectonic models*

The Boquerón and Quinini thrusts, with a regional dip of about 30° to the east and a westerly plunge, form the main structure of the Guando oilfield [3]. The westernmost segment of the faults overlies and seals the productive units that define the main underlying targets (Figure 5). The thrusting is a consequence of the Andean compressional tectonics and is the main tectonic feature of the Guando oilfield [31,34,36].

Previous 2D interpretations considered the Boquerón thrust with its detachment surface as having local spatial arrangements on the western margins, with dips that vary markedly with respect to the regional trend. These previous interpretations of the surfaces of the Boquerón thrust show an inverted dip to the west, or even typical listric upward concave buckling.

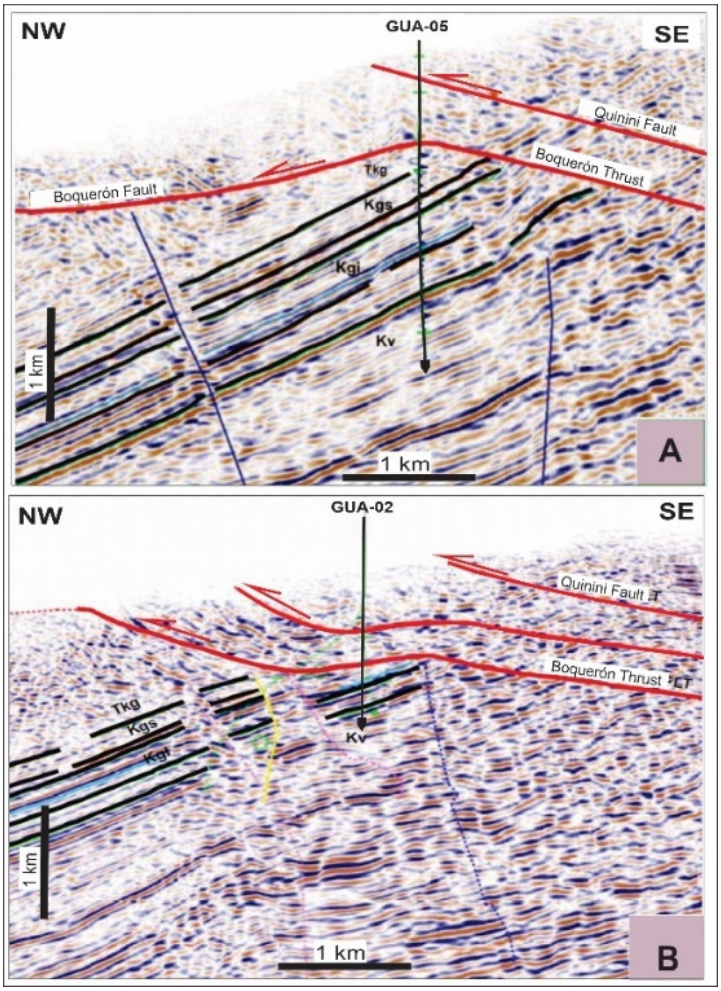


**Figure 5.** Examples of interpretations prior to the present work. A, B. 2D seismic lines (PSTM), with synthetic traces of producing wells in reservoir levels (Kg: Guadalupe sandstones; Kv: Villeta limestones; Kgi: Lower Guadalupe sandstones; Kgs: Upper Guadalupe sandstones; Tkg: Guaduas sandstones) that dip to the northwest, located in the lower block of the Boquerón thrust (taken from [3,8]). See location in Figure 3.

## 4. Results

### *4.1. The geometry characteristics of the Guando Slump*

Digital topographic interpretation of various views of high-precision elevation models shows the geomorphological evolution of the Guando Slump (Figure 6). The volume of rock affected by the slump covers the oilfield and affects the production activity. The surface shows soft reliefs that slowly move westward from the very well-marked semicircular eastern escarpment over the steep slope that marks the current watershed, arranged sub-meridionally between Icononzo and Melgar towns. At the latter locality, the most distal position of the foot of the Guando Slump can be recognized (Figure 6). The crescent length of the escarpment reaches 10 km, and the gravitational slip to its anterior foot averages about 20 km, determining a topographic slope of the order of 15°.

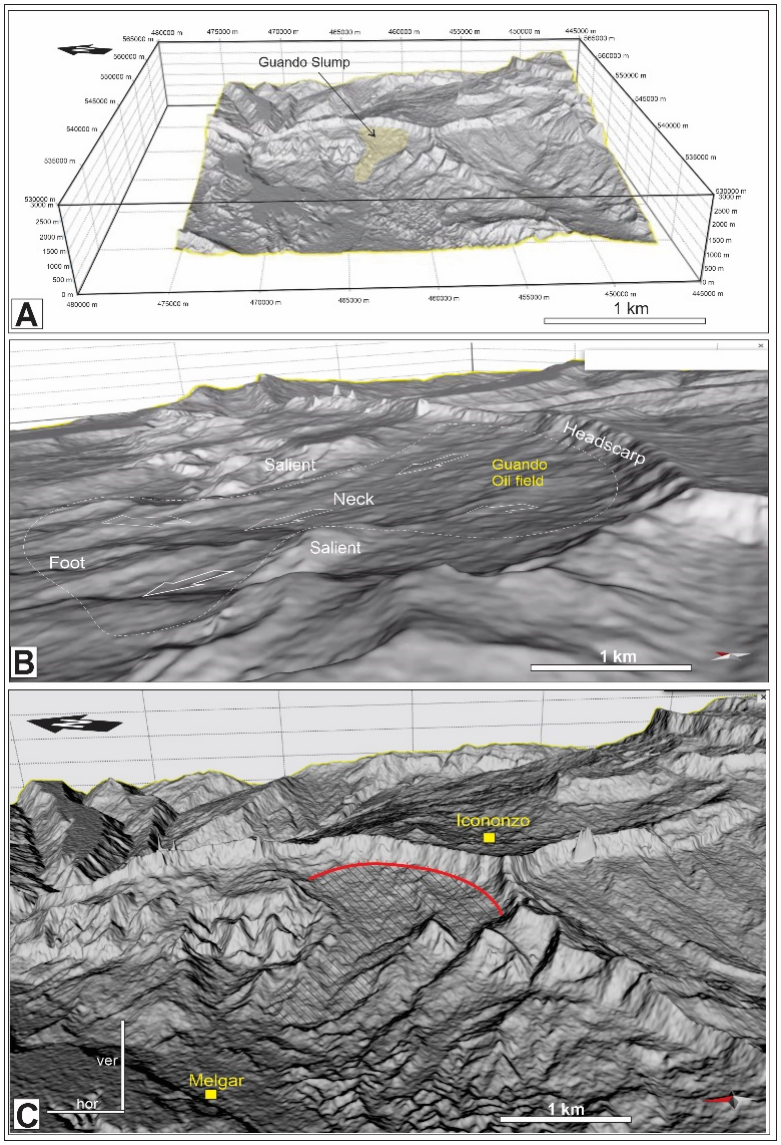


**Figure 6.** Topographic diagrams of the Guando Slump from digital models of SRTM satellite images. **A**. 3D view to the east. The red line shows the base of the escarpment. **B**. North-flush view. **C**. Frontal view to the east with indication of the sector occupied by the landslide.

From the point of view of subsurface interpretation using available seismic data, the Guando Slump is a sedimentary volume that overlies the undisturbed sequences of the oil-producing targets (sedimentary reservoirs in the Caballos, Villeta, and Guadalupe groups). This landslide has a well-marked basal detachment surface with a listric trough design in profile and the appearance of a concave crescent in plan that joins the escarpment of the topographic ridge to the east. The Guando Slump covers about 10 $km^2$ with a longitudinal extension of about 3 km and a width that varies between 1200 m and 700 m at its midpoint neck due to the interference of more resistant salients (Figure 6).

Based on the change in position of the Boquerón thrust in the slumping volume with respect to its original position in the undeformed eastern block, its displacement can be estimated to be between 1 and 2 km (Figure 7). The magnitude of the displacement is related to the regional topographic

gradient and the volume and deformability of the rocks involved in the gravitational slip. The greater the slope and the greater the deformability of the rocks involved, the greater the displacement.

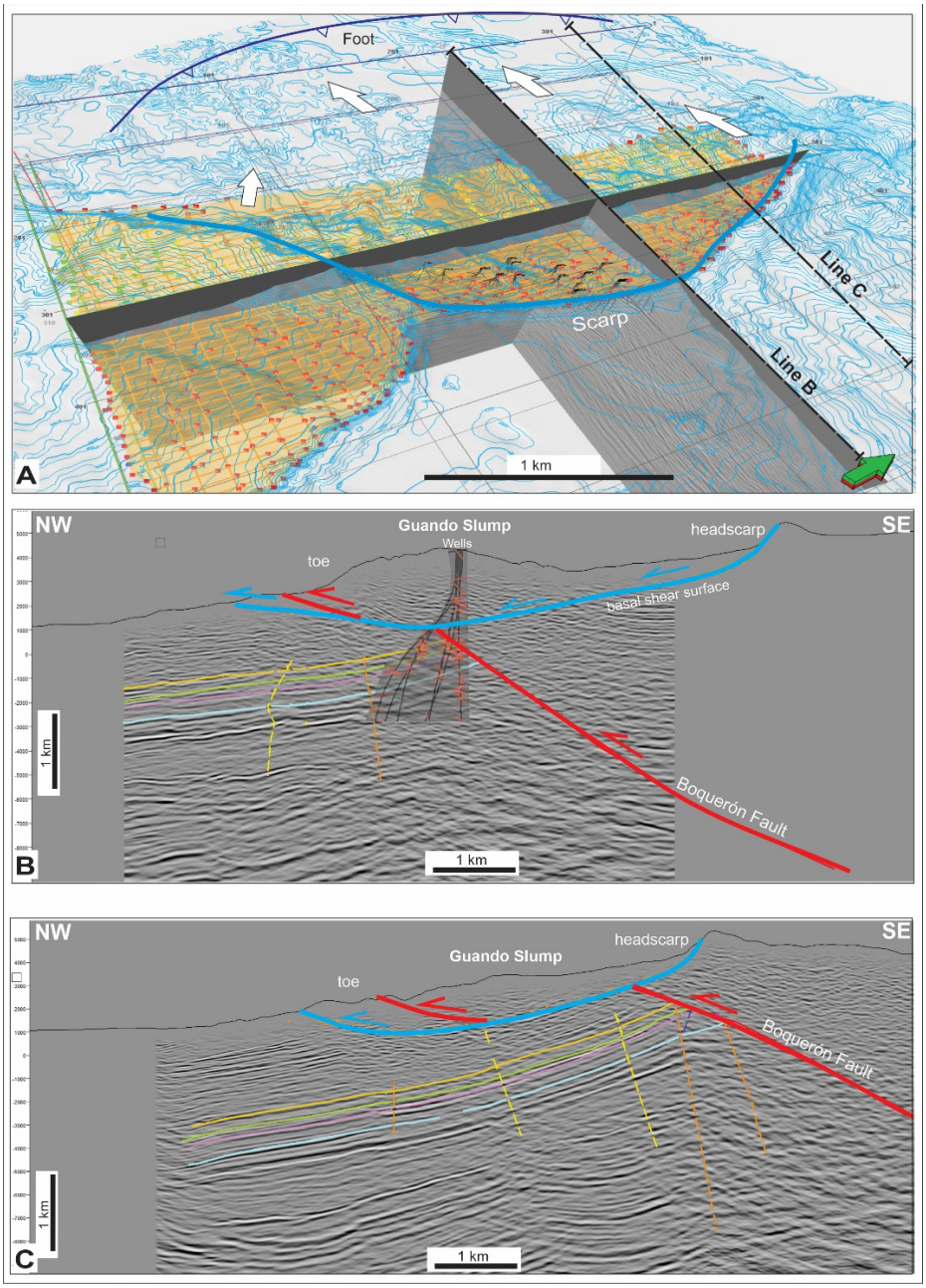


**Figure 7.** 3D projected view showing the listric geometry of the morphostructural features of the basal surface of the landslide (blue line). **A**, **B**. Interpretative transects of the Boquerón thrust (red line) partially dissected and translated NW wards by the landslide surface (taken from [8]).

Borehole image log data showing the spatial arrangement of discontinuities confirms that above the plane of the Boquerón thrust, planar features attributed to fractures with random angles and directions show no characteristic pattern. The same behavior is observed at stratigraphic boundaries where azimuths and dips are chaotic. For this reason, the geometric and temporal characterization of

the morphology of the Guando Slump detachment surface is fundamental for the design of exploration activities, the location of logistic facilities, and the orientation of future production wells.

The magnitude of slump displacement can be calculated from the relationship between the topographic relief of the landslide detachment surface [13,38–41]. In the case of the Guando Slump, the detachment in the central part of the landslide is estimated to be about 2 km, based on the lateral displacement of the Boquerón thrust. This could be due to the more intense internal disturbance of the landslide volume as it passes the threshold of the take-off surface, which favors an internal disturbance that makes it less competent and therefore more prone to collapse and erosion.

### *4.2. Structural model of the Boquerón thrust*

Previous interpretations of the westernmost segment of the Boquerón thrust in the Guando oilfield showed different surface dispositions where the horizontal maximum principal stress was not considered to be responsible for it (Figure 5). This segment shows an almost sub-horizontal laying surface, but in the easternmost segment, it is contrasted by the regional dipping toward the east (Figure 5). This discrepancy between the morphological features in the sector currently affected by the Guando Slump is very much at odds with the mechanistic underpinnings of the 4D structural interpretation.

Thus, the previously interpreted peculiar geometry of the Boquerón thrust (Figure 7) is due to the fact that its western and shallower segment was reactivated by the underlying detachment of the slumping plane. Consequently, this western segment is a part of the Boquerón thrust that has been modified and displaced by the slip plane. For this reason, from the seismic data, it appears to be associated with the same surface, giving the appearance of conforming to the same and continuous structure.

On the other hand, if the western part of the Boquerón thrust was, as previously proposed, a thrust, it would have to be east-vergent to respect the unambiguous spatial relationships between faulting and stress fields [see a synthesis in 42]. This relationship determines that the maximum principal stress $\sigma_1$ and the fault surfaces will always maintain an angle of less than 45°, often of the order of 30°–40°. Therefore, regardless of whether it is a normal, reverse, or transcurrent fault, the maximum principal stress $\sigma_1$ is always located at an angle of less than 45° (close to 30°–40°) with respect to the fault plane on which it acts (Figure 8).

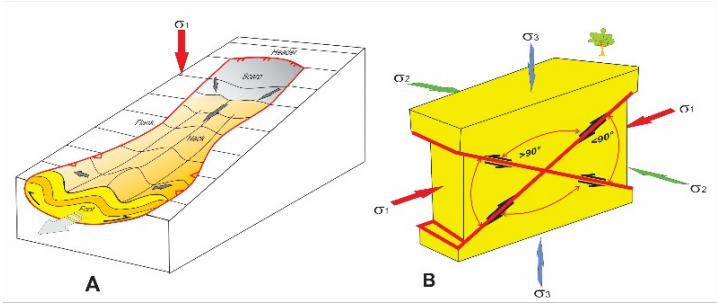


**Figure 8**. **A**: Schematic representation of the typical relationship between the vertical position of the maximum principal stress in a slumping whose displacement is sub-horizontal. **B**: Schematics of Anderson's law, which establishes univocal spatial relationships between the stress field and thrusting always at < 45° (modified from [42]).

Therefore, if the previous interpretations are maintained, it would be an anomalous situation to consider that the same surface of the Boquerón thrust has opposite vergences, as shown in Figure 5.

## 5. Discussion

The multi-lithological Cretaceous sequences of the Villeta Group of the Guando oilfield have different mechanical responses, allowing the identification of detachment surfaces that exploit mechanical discontinuities for their development. This active slumping in mountainous regions with rugged relief, humid weather, and seismicity defines a westward sliding hanging block above the undisturbed oil target sequences. This horizontal displacement of 1–2 km provides a coherent explanation for the mechanical problems encountered by production and injection wells crossing it. These collapse and/or throttling problems increase with the age of the wells.

Based on various antecedents [43–45], the triggering of the Guando Slump gravity process may have been favored by the combination of steep relief and the interaction of the following causes:

- High regional tectonic instability in the midst of the developing and rapid exhumation of the Central Cordillera, which affects the readjustment of the base level. The stability conditions in the pre-rupture phase are assessed taking into account the initial geometry of the slope, the strength limit of the materials involved, the groundwater and/or percolation conditions, and the effect of possible external forces (earthquakes, overloads, excavations, etc.).
- Intense weathering contributes to the erosion processes due to climate and abrupt changes in the ground level.
- The multi-compositional nature of the affected volume of rocks with interspersed incompetent levels, particularly the plasticity of the interfinger pelites and mechanical equivalent rocks of the Cretaceous Villeta Group. This incompetent behavior acts as a lubricant capable of defining a detachment surface that triggers gravitational displacement.

The evolution of the Guando Slump can be explained as a recent and still evolving feature affecting the Boquerón thrust, giving it the particular listric geometry previously interpreted (Figure 9).

The curved structures with opposite dips at the western end with respect to the interpreted regional spatial trend in their eastern continuity were inconsistent with the mechanistic underpinnings of the 4D structural interpretation. This is because they do not conform to Anderson's law, which establishes a certain angular relationship between the orientation of the generating stress field and the produced fault surfaces [42,46,47].

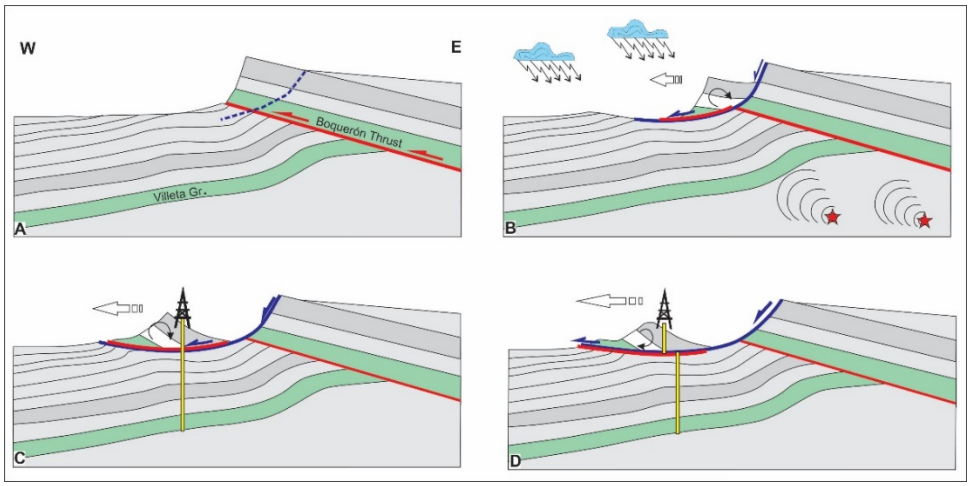


**Figure 9.** Schematic evolution of gravitational slip on the Boquerón fault and its overhanging slip compartment from conceptual sections. **A**. Previous state, with the position of the potential slip plane indicated. **B**. Slip initiation triggered by seismicity (red stars) and weathering favored by the mechanical inconsistency of Villeta Group pelites. **C**. An advanced landslide where a producing well is located. **D**. Current state where the collapse of the producing well can be seen.

Moreover, this gravitational slip, which developed over the Guando oilfield, could explain the problems of pipe collapse due to tangential deformation at depths compatible with its location and the presence of hydrocarbons in shallow and variably disturbed reservoirs, which must have been loaded prior to its operation.

Unfortunately, a calculation of the displacement velocity is not yet available, which could be made from different methodologies applied in other cases [48–50]. If information on the speed of gravitational movement of the Guando Slump were available, it would be possible to implement measures to mitigate the catastrophic effects of displacements [51,52]. In this way, they could be taken into account in the siting of the infrastructure to estimate its useful life and possible attenuation in the case of wells that will have to cross the basal surface of the displacement.

The measures to mitigate the consequences of landslides are clearly different before and after the failure. In the pre-failure phase, the potential instability must be assessed in its geological context in order to determine the measures to be taken to protect and/or contain the slope movement. In the event of an overt failure, various measures must be taken, ranging from immediate evacuation if necessary and feasible to containment and remediation. The techniques and procedures to be employed will be specific to each phase and will require a differentiated approach.

## 6. Conclusion

This detailed 3D surface and subsurface study in the Guando oil field identified the active landslide phenomenon represented by the Guando Slump and a new structural interpretation of the Boquerón thrust.

The new tectonic model significantly modifies the previous structural model based on the Boquerón thrust, due to the strong incompatibility of the spatial relationship between the westernmost

segment of the Boquerón thrust and the responsible stress fields. The previously assumed position of the westernmost segment of the Boquerón thrust is strongly modified by a gravitational slip, which causes the initial layout of its surface to be strongly obliterated. This structural model provides new observations and a more confident interpretation that takes into account the integral characteristics of the Boquerón thrust and the active deformation events due to the Guando slump.

The spatial and temporal diversity of the structures detected in the Guando oilfield hinders the application of geometrically balanced reconstruction techniques that consider all events in a single process; therefore, a multiscale and evolutionary tectonic analysis is required.

Finally, the structural peculiarities of the tectonic model of the Guando oilfield, due to the presence of the active Guando Slump, if properly monitored, can contribute to a better management of the oilfield.

## Use of Generative-AI tools declaration

The authors declare they have not used Artificial Intelligence (AI) tools in the creation of this article.

## Acknowledgements

Thoughtful discussions with colleagues, particularly Ing. José L. Saavedra, both in the office and in the field at Petrobras Colombia, have improved the understanding of the geological and geophysical aspects of the Guando oilfield and the Upper Magdalena Valley Basin. Ing. Juan Badillo assisted in the preparation of the DEM. The editorial treatment of the manuscript by two anonymous reviewers is highly appreciated as it has improved the quality and clarity.

## Conflict of interest

The author declares no conflicts of interest in this paper.

## References

1. Buitrago J (1994) Petroleum systems of the Neiva Area, Upper Magdalena Valley, Colombia. In: Magoon LB, WG Dow (eds.), The Petroleum System – from source to trap. *AAPG*, *Memoir* 60: 483–497. https://doi.org/10.1306/M60585C30
2. Mojica J, Franco R (1990) Estructura y evolución tectónica del Valle Medio y Superior del Magdalena, Colombia. *Geol Colombiana* 17: 41–64.
3. Rincón G, Garzón JC, de Moraes JJ (2003) Campo Guando, Primer Descubrimiento de la Antesala del Siglo XXI en el Valle Superior del Magdalena, Colombia. 8th Simposio Bolivariano - Exploración Petrolera en las Cuencas Subandinas. Cartagena, Colombia. https://www.earthdoc.org/content/papers/10.3997/2214-4609-pdb.33.Paper66
4. Sarmiento LF, Rangel A (2004) Petroleum systems of the Upper Magdalena Valley, Colombia. *Mar Petrol Geol* 21: 373–391. https://doi.org/10.1016/j.marpetgeo.2003.11.019
5. Ramón J, Rosero A (2006) Multiphase structural evolution of the western margin of the Girardot Subbasin, Upper Magdalena Valley, Colombia. *J S Am Earth Sci* 21: 493–509. https://doi.org/10.1016/j.jsames.2006.07.012

6. Barrero D, Pardo A, Vargas CA, et al. (2007) Colombian sedimentary basins: nomenclature, boundaries and petroleum geology, a new proposal. Agencia Nacional de Hidrocarburos - B&M Exploration Ltda. 35pp. Bogotá.
7. Roncancio J, Martínez M (2011) Upper Magdalena Basin. *In*: Cediel F, Colmenares F (eds.), Petroleum Geology of Colombia. Fondo Editorial Universidad Eafit, vol. 14: 183 pp. Medellin.
8. Rossello EA, Saavedra JL (2020) El deslizamiento gravitatorio de Guando (Tolima, Colombia): características morfoestructurales y consecuencias de su interpretación. *Bol Geol* 42: 151–170. https://doi.org/10.18273/revbol.v42n3-2020007
9. Arévalo-Chaves DA, Parias-Villalba JP (2013) Análisis de amenaza por fenómenos de remoción en masa en la región del Boquerón ubicada entre los departamentos de Cundinamarca y Tolima mediante el uso de un Sistema de información geográfica de libre distribución. Tesis, Universidad Católica de Colombia, Bogotá, Colombia, 73.
10. Pfiffner OA (2017) Thick-skinned and thin-skinned tectonics: A global perspective. *Geosciences* 7: 1–89. https://doi.org/10.3390/geosciences7030071
11. Nemčok A, Pašek J, Rybář J (1972) Classification of landslides and other mass movements. *Rock Mechanics* 4: 71–78. https://doi.org/10.1007/BF01239137
12. Hutchinson JN, Bhandari RK (1971) Undrained loading, a fundamental mechanism of mudflows and other mass movements. *Géotechnique* 21: 353–358. https://doi.org/10.1680/geot.1971.21.4.353
13. Varnes DJ (1978) Slope movement types and processes. In: Schuster RL, Krizek RJ (eds.), Landslides, analysis and control. *Transportation research board, National Academy of Sciences*. Special report 176: Chapter 2: 11–33. https://trid.trb.org/view/86168
14. Crozier MJ (1986) Landslides: causes, consequences and environment. Croom Helm. 252. London, https://doi.org/10.1080/03036758.1988.10429158
15. Cruden DM, Varnes DJ (1996) Landslide types and processes. In: Turner AK, Schuster RL (eds.), Landslides investigation and mitigation. US National Research Council. Special Report 247, Chapter 3: 36–75.
16. Dikau R, Brunsdsen D, Schrott L, et al. (1996) Landslides recognition: identification, movement and causes. John Wiley & Sons. 274.
17. Leroueil S, Locat J, Vaunat J, et al. (1996) Geotechnical characterization of slope movements. In: Senneset K (ed.), Landslides. Balkema, Rotterdam 1: 53–74.
18. Sassa K (1999) Introduction. In: Sassa K (ed.), Landslides of the world. Kyoto University Press. 3–18. https://doi.org/10.1007/3-540-27129-5_5
19. Alcántara-Ayala I (2000) Landslides: ¿deslizamientos o movimientos del terreno? Definición, clasificaciones y terminología. Investigaciones Geográficas: Boletín – Instituto de Geografía, Universidad Nacional Autónoma de México, 41: 7–25. https://doi.org/10.14350/rig.59101
20. Alsop GI, Marco S, Weinberger R, et al. (2017) Upslope-verging back thrusts developed during downslope-directed slumping of mass transport deposits. *J Struct Geol* 100: 45–61. https://doi.org/10.1016/j.jsg.2017.05.006
21. Easterbrook DJ (1993) Surfaces processes and landforms. 2nd Ed. Prentice Hall. Nueva York, 230.
22. Glade T, Anderson M, Crozier MJ (2012) Landslide hazard and risk. John Wiley & Sons. Chichester, 807. https://doi.org/10.1002/9780470012659
23. Ng KS, Chew YM (2019) Slope stability analysis of embankment over stone column improved ground. *J Eng Sci Technol* 14: 3582–3596.

24. Hennings P, Olson J, Thompson L ( 2000) Combining outcrop data and three-dimensional structural models to characterize fracture reservoirs: an example from Wyoming. *AAPG Bulletin* 84: 830–849. https://doi.org/10.1306/A967340A-1738-11D7-8645000102C1865D
25. Hergarten S, Robl J, Stüwe K (2014) Extracting topographic swath profiles across curved geomorphic features. *Earth Surf Dynam* 2: 97–104. https://doi.org/10.5194/esurf-2-97-2014
26. Jaimes E, De Freitas M (2006) An Albian-Cenomanian unconformity in the Northern Andes: Evidence and tectonic significance. *J S Am Earth Sci* 21: 466–492. https://doi.org/10.1016/j.jsames.2006.07.011
27. Mantilla M, Salazar CC, Rossello EA (2024) The geology of the La Hocha High and its associated oil fields (southern Upper Magdalena Valley, Colombia): a new 3D structural model based on 3D subsurface data. *Geociências* 43: 537–557. https://doi.org/10.5016/geociencias.v43i4.18579
28. Cediel F, Mojica J, Macía C (1981) Definición estratigráfica del Triásico de Colombia, Suramérica. Las Formaciones Luisa, Payandé, Saldaña. Sus columnas estratigráficas. *Newsl Stratigr* 9: 73–104. https://doi.org/10.1127/nos/9/1980/73
29. Horton BK, Parra M, Mora A (2020) Construction of the Eastern Cordillera of Colombia: Insights from the sedimentary record. In: Gómez J, Mateus-Zabala D (eds.), The Geology of Colombia, Volume 3 Paleogene – Neogene. *Servicio Geológico Colombiano*, Publicaciones Geológicas Especiales 37: 67–88. Bogotá. https://doi.org/10.32685/pub.esp.37.2019.03
30. Cobbold PR, Davy P, Gapais D, et al. (1993) Sedimentary basins and crustal thickening. *Sediment Geol* 86: 77–89. https://doi.org/10.1016/0037-0738(93)90134-Q
31. Schamel S (1991) Middle and Upper Magdalena Basins, Colombia. In: Biddle KT (ed.), Active margin basin. *AAPG, Memoir*, 52. Chapter 10: 283–301. https://doi.org/10.1306/M52531C10
32. Cooper MA, Addison FT, Alvarez R, et al. (1995) Basin development and tectonic history of the Llanos Basin, Eastern Cordillera and Magdalena Valley, Colombia. *AAPG Bulletin* 79: 1421–1443. https://doi.org/10.1306/7834D9F4-1721-11D7-8645000102C1865D
33. Toro J, Roure F, Bordas-Le Floch N, et al. (2004) Thermal and kinematic evolution of the Eastern Cordillera fold and thrust belt, Colombia. In: Swennen R et al. (eds.), Deformation, fluid flow, and reservoir appraisal in foreland fold and thrust belts. *AAPG, Hedberg Series*, 1: 79–115. https://doi.org/10.1306/1025687H13114
34. Sarmiento-Rojas LF, Van Wess JD, Cloetingh S (2006) Mesozoic transtensional basin history of the Eastern Cordillera, Colombian Andes: Inferences from tectonic models. *J S Am Earth Sci* 21: 383–411. https://doi.org/10.1016/j.jsames.2006.07.003
35. Mora-Páez H, Mencin, DJ, Molnar P, et al. (2016) GPS velocities and the construction of the Eastern Cordillera of the Colombian Andes. *Geophys Res Lett* 43: 8407–8416. http://doi.org/10.1002/2016GL069795
36. Rossello EA, Gallardo A (2022) The Sierra Nevada de Santa Marta (Colombia) and Nevado de Famatina (Argentina) positive syntaxes: two comparable exceptional relieves in the Andes foreland. *J Struct Geol* 160: https://doi.org/10.1016/j.jsg.2022.104618
37. Cobbold PR, Rossello EA, Roperch P, et al. (2007) Distribution, timing, and causes of Andean deformation across South America. *Geological Society, London, Special Publications* 272: 321–343. https://doi.org/10.1144/GSL.SP.2007.272.01.17
38. Lewis KB (1971) Slumping on a continental slope inclined at 1–4°. *Sedimentology* 16: 97–110. http://doi.org/10.1111/j.1365-3091.1971.tb00221.x

39. Martinsen OJ (1994) Mass movements. In: Maltman A (ed.), The geological deformation of sediments. Chapman & Hall, London, 27–165. http://doi.org/10.1007/978-94-011-0731-0_5
40. Bull S, Cartwright J, Huuse M (2009) A review of kinematic indicators from mass-transport complexes using 3D seismic data. *Mar Petrol Geol* 26: 1132–1151. http://doi:10.1016/j.marpetgeo.2008.09.011
41. Sobiesiak MS, Kneller B, Alsop GI, et al. (2018) Styles of basal interaction beneath mass transport deposits. *Mar Petrol Geol* 98: 629–639. http://doi.org/10.1016/j.marpetgeo.2018.08.028
42. Rossello EA, López-Isaza JA (2023) The structural control of mineralizations by dilatancies due to differential thermal expansivity (in disseminated deposits) and faults bending (in veins): revision and working hypothesis. *Rev Mex Cienc Geol* 40: 16–34. http://dx.doi.org/10.22201/cgeo.20072902e.2023.1.1716
43. Gostelow TP (1991) Rainfall and landslides. In: Almeida-Teixeira F et al. (eds.), Prevention and control of landslides and other mass movements. Commission of the European Communities. Report EUR 12918: 139–161.
44. Girty GH (2009) Perilous Earth: Understanding processes behind natural disasters. Chapter 7, 1–17, Montezuma Publishing, San Diego. Available from: https://studylib.net/doc/8423341/chapter-1.
45. Hungr O, Leroueil S, Picarelli L (2013) The Varnes classification of landslide types, an update. *Landslides* 11: 167–194. https://doi.org/10.1007/s10346-013-0436-y
46. Ramsay JG, Huber MI (1983) The techniques of modern structural geology: strain analyses. Academic Press. 393.
47. Price NJ, Cosgrove JW (1990) Analysis of geological structures. Cambridge University Press. 502.
48. Working Party for World Landslide Inventory (1995) A suggested method for describing the rate of movement of a landslide. *Bulletin of the International Association of Engineering Geology* 52: 75–78. https://doi.org/10.1007/BF02639593
49. Tofani V, Raspini F, Catani F, et al. (2013) Persistent Scatterer Interferometry (PSI) technique for landslide characterization and monitoring. *Remote Sens* 5: 1045–1065. https://doi.org/10.3390/rs5031045
50. Tiampo KF, González PJ, Samsonov SS (2013) Results for aseismic creep on the Hayward fault using polarization persistent scatterer InSAR. *Earth Planet Sc Lett* 367: 157–165. https://doi.org/10.1016/j.epsl.2013.02.019
51. Záruba Q, Mencl V (1969) Landslides and their control. Elsevier. Amsterdam, 270.
52. Schuster RL, Salcedo DA, Valenzuela L (2002) Overview of catastrophic landslides of South America in the twentieth century. In: Evans SG, DeGraff JV (eds.). Catastrophic Landslides: effects, occurrence, and mechanisms The Geological Society of America. *Reviews in Engineering Geology*, XV: 1–34. https://doi.org/10.1130/REG15-p1



AIMS Press